Electronic Supplementary Material (ESI) for Journal of Materials Chemistry A.

Supporting Information

Highly stable and uniformly dispersed 1T-MoS_2 nanosheets co-induced by chemical pressure and 2D template method with high supercapacitor performance

Han Li[a,b], Shuai Lin[*a], Hui Li[a,b], Ziqiang Wu[a,b], Lili Zhu[a,b], Changdian Li[a,b], Xuebin Zhu[*a,b], Yuping Sun [a,c,d]

[a] Key Laboratory of Materials Physics, Institute of Solid State Physics, HFIPS, Chinese Academy of Sciences, Hefei 230031, People's Republic of China

[b] University of Science and Technology of China, Hefei 230026, People's Republic of China

[c] High Magnetic Field Laboratory, HFIPS, Chinese Academy of Sciences, Hefei 230031, People's Republic of China

[d] Collaborative Innovation Center of Advanced Microstructures, Nanjing University, Nanjing 210093, People's Republic of China

***Corresponding authors E-mail:** linshuai17@issp.ac.cn; xbzhu@issp.ac.cn

List of Texts, Figures and Tables

ethanedioic acid dehydrate.

Figure S14. CV and GCD curves of 1T-MWS/$Ti_xC_2T_x$ MXene-11, 1T-MWS/$Ti_xC_2T_x$ MXene-55 and 1T-MWS/$Ti_xC_2T_x$ MXene-220.

Figure S15. The Specific capacitance of all samples at different current densities.

Figure S16. The EIS of 1T-MWS/$Ti_xC_2T_x$ MXene-11, 1T-MWS/$Ti_xC_2T_x$ MXene-55 and 1T-MWS/$Ti_xC_2T_x$ MXene-220.

Figure S17. The CV curves of all samples.

Figure S18. The GCD curves of all samples.

Figure S19. The b values of 1T-MWS/$Ti_3C_2T_x$ MXene-11, 1T-1T-MWS/$Ti_3C_2T_x$ MXene-55 and 1T-MWS/$Ti_3C_2T_x$ MXene-220.

Figure S20. The SEM images and XRD pattern of 1T-MWS/$Ti_3C_2T_x$ MXene-110 electrodes before and after long-term cycling.

Figure S21. Digital photographs of the symmetric all-solid-state supercapacitors devices bent at different angles of 0°, 30°, 60° and 90° at 20 mV s^{-1}.

Table S1. The specific capacitance of all samples.

Table S2. The areal capacitance, mass capacitance, energy and power density of the ASSSs devices at different current densities.

Table S3. Comparisons of energy and power density of 1T-MWS/$Ti_3C_2T_x$ MXene-110 based flexible ASSSs with those of advanced flexible devices reported recently.

Text S1. Experimental section

Chemicals: Ammonium molybdate tetrahydrate ($(NH_4)_6Mo_7O_{24}\cdot 4H_2O$), thiourea ($CH_4N_2S$) and powder of Al (99.9%; -325 mesh) were purchased from Alfa Aesar. Powder of Ti (99.9%; -200 mesh) and HF were purchased from Aladdin. Powder of C, ammonium tungstate hydrate ($(NH_4)_{10}W_{12}O_{41}\cdot xH_2O$), ethanedioic acid dihydrate ($C_2H_2O_4\cdot 2H_2O$), anhydrous sodium sulfatewere (Na_2SO_4) and potassium chloride (KCl) were purchased from Sinopharm Chemical Reagent Co. Ltd. (Shanghai, China). All chemicals were used without any further purification.

Preparation of $Ti_3C_2T_x$ MXene: Ti powder, Al powder and C powder were mixed in a ratio of 3: 1.1: 2, then ball milled for 1 hour to obtain a uniformly mixed powder. The obtained powder was pressed into cylindrical particles with a diameter of 13 mm under the pressure of 1 GPA. Place the particles in a tube furnace at a heating rate of 9°C/minute, heating up to 1000°C, and then heating up to 1400°C Celsius at a heating rate of 5°C/minute for 2 hours under a constant flow of argon. After the sample is cooled to room temperature, it is manually ground and crushed into powder. Add 40% HF slowly to the sample and continue stirring for 24 hours. In the case of centrifugation, repeated washing with deionized water until the pH value of the supernatant exceeded 6, and the resulting black product is placed in a vacuum drying oven for 12 hours.

Preparation of 1T-MWS: 0.2897 g $(NH_4)_6Mo_7O_{24}\cdot 4H_2O$, 1.4209 g CH_4N_2S and 0.6240 g $(NH_4)_{10}W_{12}O_{41}\cdot xH_2O$ are dissolved in 21.8 ml deionized water and stirred for 30 min. The homogeneous mixture was transferred into a 28 ml Teflon reactor and reacted 210°C for 18 hours, then cool dawn to room temperature. The resulting product

was washed with deionized water and ethanol for several times followed by dying at 60°C at vacuum oven.

Preparation of 1T-MWS/$Ti_xC_2T_x$ MXene heterostructure: $(NH_4)_6Mo_7O_{24}\cdot 4H_2O$, CH_4N_2S and $(NH_4)_{10}W_{12}O_{41}\cdot xH_2O$ are dissolved in 21.8 ml deionized water (the usage is consistent with the preparation of 1T-$Mo_{0.4}W_{0.6}S_2$), then 0.2068 g $C_2H_2O_4\cdot 2H_2O$ and three diffident qualities (0.011, 0.055, 0.11 and 0.22 g) of $Ti_3C_2T_x$ are added into the above mixed solution, kept stirring. The homogeneous mixture was transferred into a 28 ml Teflon reactor and reacted 210°C for 18 hours, then the following process is consistent with the preparation of 1T-MWS.

Text S2. Material characterizations

XRD spectra were collected on Philips X′pert PRO X-ray diffractometer with Cu K radiation (λ = 0.15406 nm). Raman spectra were obtained by a LabRAMHR800 UV NIR spectrometer with 532 nm laser excitation. Fourier transform infrared (FTIR) spectra were obtained on a NEXUS 750 spectrometer using the KBr pellets in the range of 4000-400 cm^{-1}. N_2 adsorption/desorption measurements of samples were carried out using ASAP2460 Version 3.01. The specific surface areas were obtained employing BrunauerEmmett-Teller (BET) method. Materials nanostructure characterizations come from Field emission scanning electron microscope (FE-SEM, Quanta 200FEG) and Energy-dispersive X-ray spectroscopy (EDS, Oxford EDS, with INCA software), transmission electron microscope (TEM, JEM-2100) with configured EDS, X-ray photoelectron spectroscopy (XPS, Thermo ESCALAB 250Xi equipped with monochromatic Al Kα source of 1486.6 eV). The HAADF-STEM and corresponding

EELS mapping analyses were performed on a JEOL JEM-ARM200F TEM/STEM (200 kV) with a spherical aberration corrector.

Text S3. Electrochemical measurements and Evaluations

Platinum electrode was used as counter electrode and Ag/AgCl in 1 M KCl electrode as reference electrode. The working electrode is mainly made of electrode material, polyvinylidene fluoride (PVDF) and conductive carbon black (super-p) according to the mass ratio of 8:1:1, and then adding the liquid of N-methylpyrrolidone (NMP) to prepare the slurry, which is obtained on the carbon paper. The area of slurry brush on carbon paper is 1cm^2, and the loading mass of the electrode material is about 1-2 mg. The electrodes were dried in vacuum oven at 50 °C for 6 hours. Electrochemical data is provided by Dutch Ivium (Vertex.C.DC) electrochemical station in 1M Na_2SO_4, so cyclic voltammetry (CV), galvanostatic charge-discharge (GCD) and electrochemical impedance spectroscopy (EIS) can be obtained.

Preparation of the Na_2SO_4/PVA gel: 1 g of PVA was dissolved in 10 ml of deionized water at 90°C. With the continuous evaporation of water, the solution is gelatinous. Add an appropriate amount of 1m Na_2SO_4 solution and continue to evaporate until it is gelatinous again.

Preparation of the symmetric flexible all-solid-state supercapacitors (ASSSs) devices: The two carbon cloth with brushing similar quality with 1×1 cm^2 area of electrode material are placed opposite to each other. Between the two electrodes, a Na_2SO_4/PVA gel with uniform thickness is brushed, and a cut cellulose separator is added in the middle. Use the packaging film to package it.

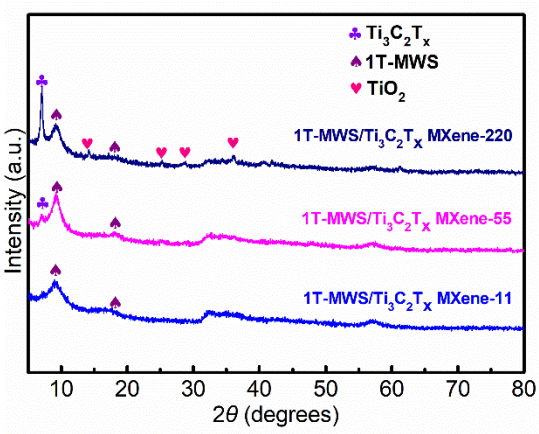

Figure S1. XRD patterns of 1T-MWS/$Ti_xC_2T_x$ MXene-11, 1T-MWS/$Ti_xC_2T_x$ MXene-55 and 1T-MWS/$Ti_xC_2T_x$ MXene-220.

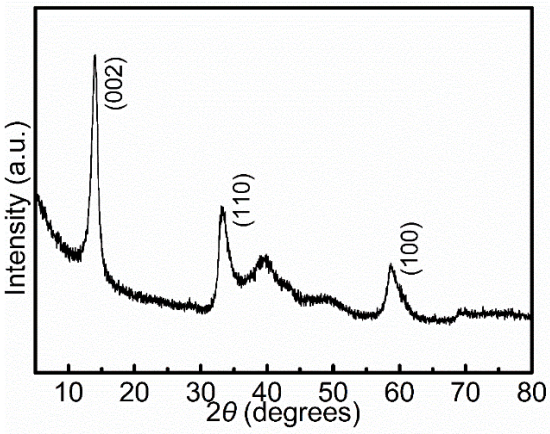

Figure S2. XRD patterns of 2H-MoS_2.

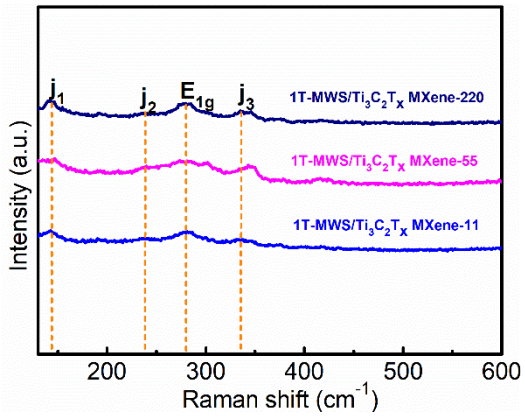

Figure S3. Raman spectrum of 1T-MWS/$Ti_xC_2T_x$ MXene-11, 1T-MWS/$Ti_xC_2T_x$ MXene-55 and 1T-MWS/$Ti_xC_2T_x$ MXene-220.

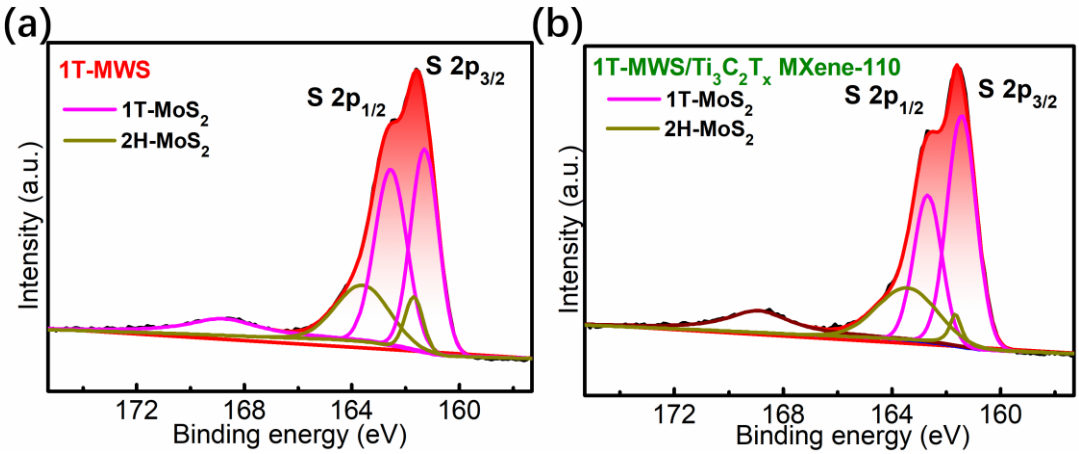

Figure S4. The S 2s XPS surveys of 1T-MWS and 1T-MWS/$Ti_xC_2T_x$ MXene-110.

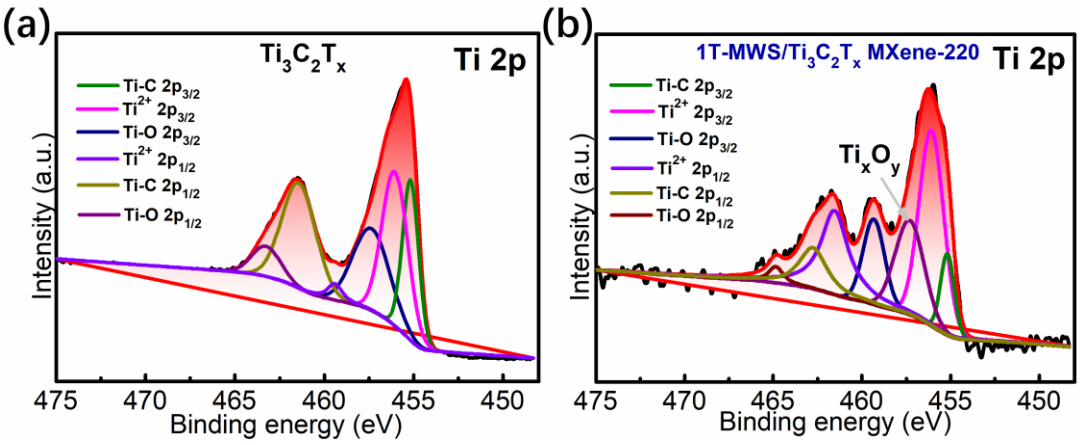

Figure S5. The Ti 2p XPS surveys of $Ti_3C_2T_x$ and 1T-MWS/$Ti_3C_2T_x$ MXene-220.

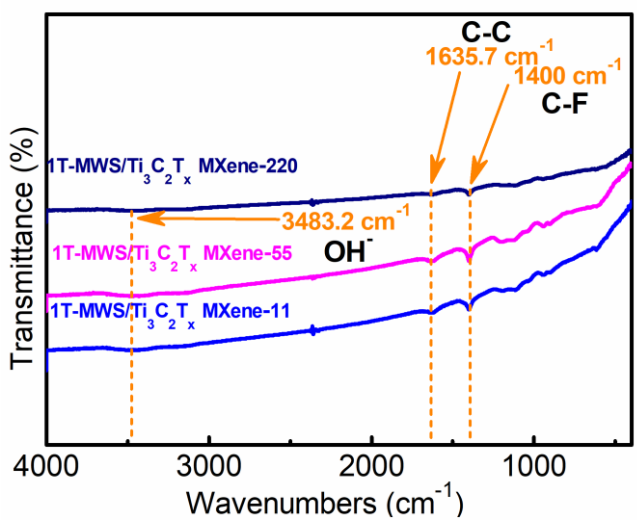

Figure S6. FTIR spectra of 1T-MWS/$Ti_xC_2T_x$ MXene-11, 1T-MWS/$Ti_xC_2T_x$ MXene-55 and 1T-MWS/$Ti_xC_2T_x$ MXene-220.

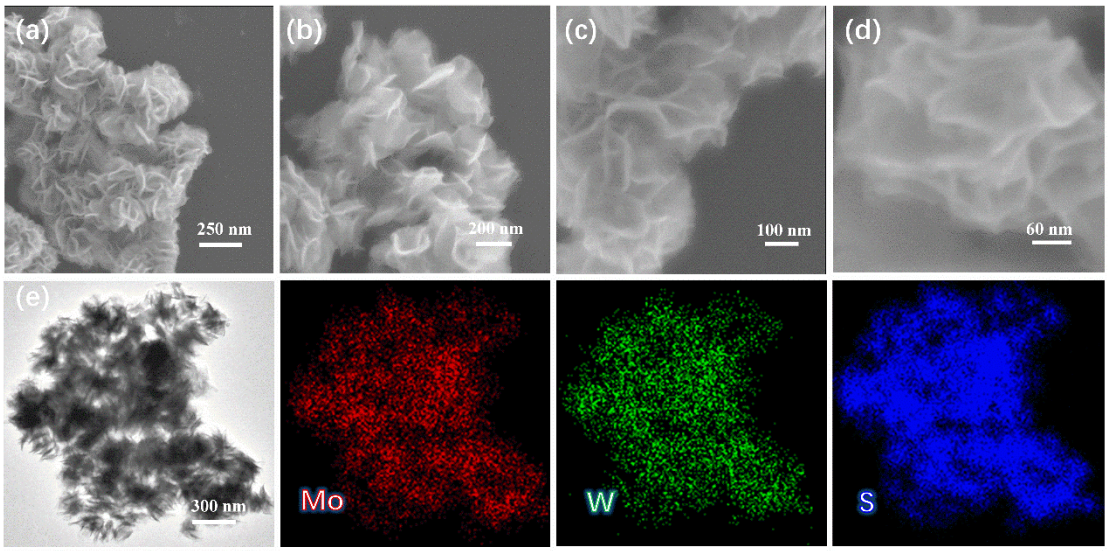

Figure S7. a-d) The SEM images of 1T-MWS. e) The EDS mapping images of Mo, W and S element.

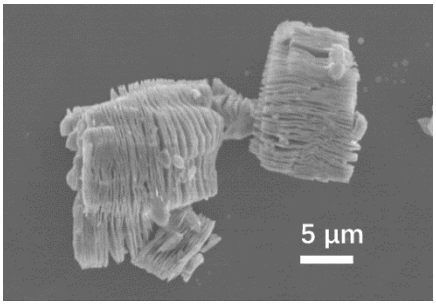

Figure S8. The SEM image of $Ti_3C_2T_x$.

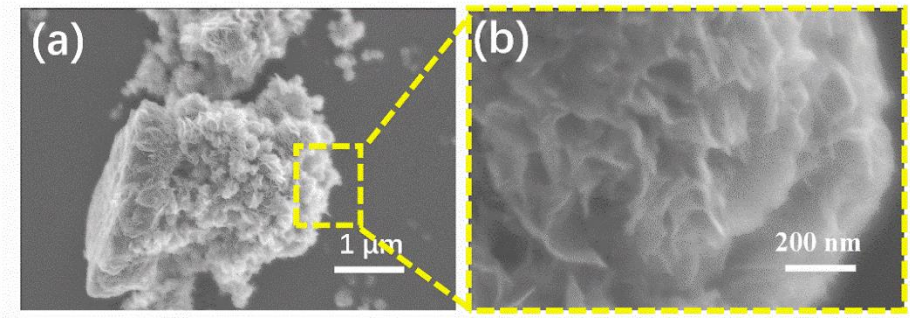

Figure S9. a-b) The SEM images of 1T-MWS/$Ti_xC_2T_x$ MXene-11.

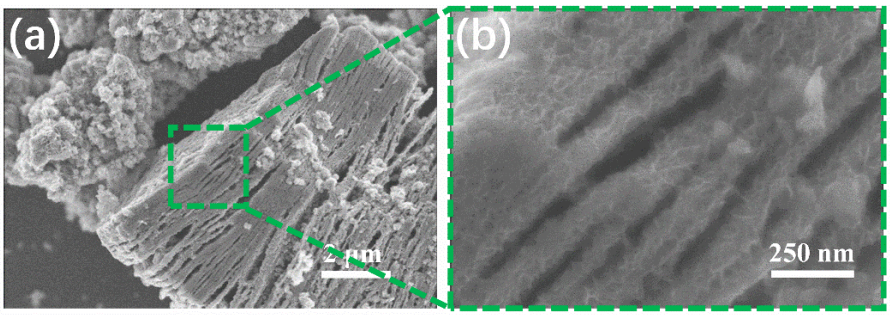

Figure S10. a-b) The SEM images of 1T-MWS/$Ti_xC_2T_x$ MXene-55.

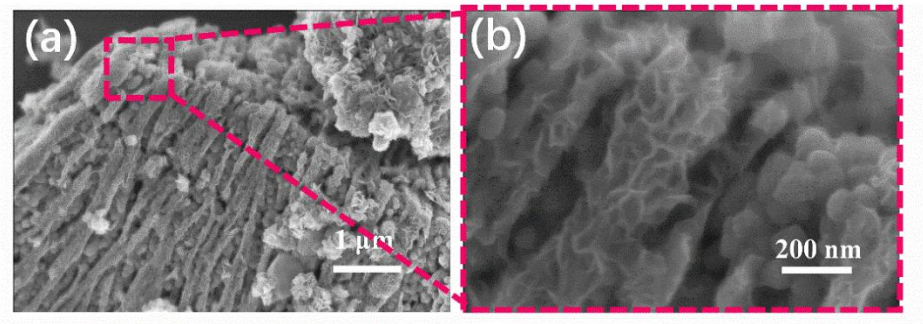

Figure S11. a-b) The SEM images of 1T-MWS/$Ti_xC_2T_x$ MXene-220.

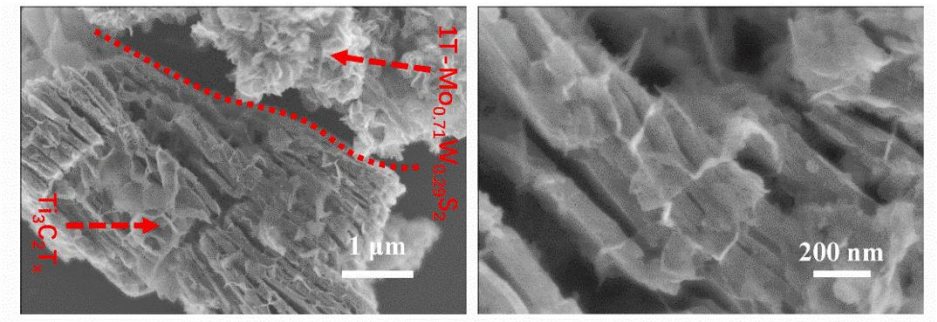

Figure S12. a-b) The SEM images of 1T-MWS/$Ti_xC_2T_x$ MXene-110 without the ethanedioic acid dehydrate.

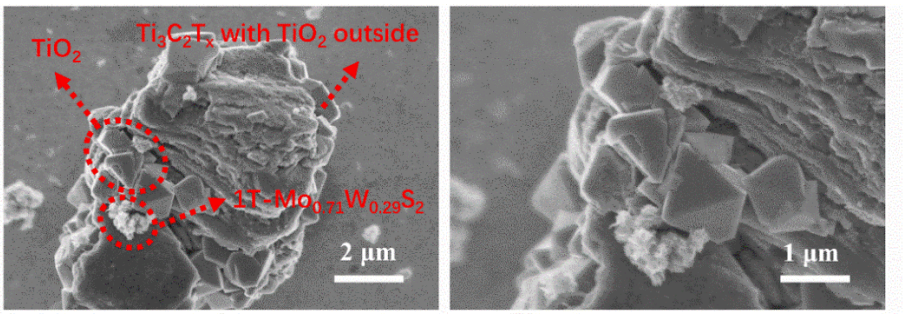

Figure S13. a-b) The SEM images of 1T-MWS/$Ti_xC_2T_x$ MXene-220 without the ethanedioic acid dehydrate.

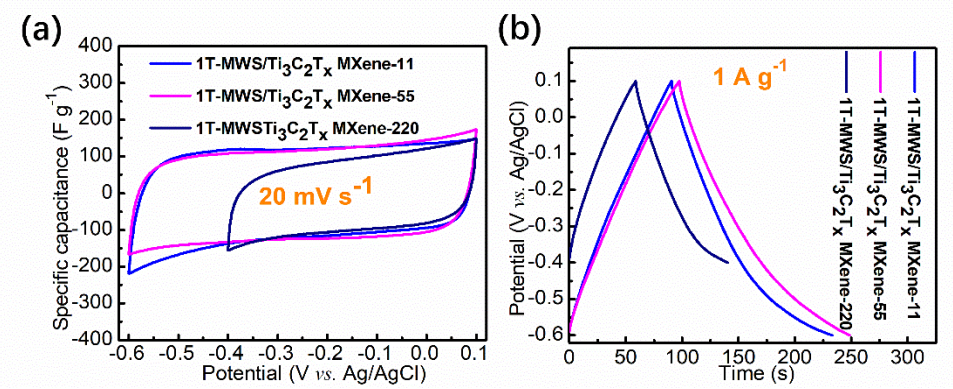

Figure S14. The CV and GCD curves of 1T-MWS/$Ti_xC_2T_x$ MXene-11, 1T-MWS/$Ti_xC_2T_x$ MXene-55 and 1T-MWS/$Ti_xC_2T_x$ MXene-220.

Table S1. The specific capacitance of all samples.

	$Ti_3C_2T_x$	1T-MWS	1T-MWS/$Ti_3C_2T_x$ MXene-11	1T-MWS/$Ti_3C_2T_x$ MXene-55	1T-MWS/$Ti_3C_2T_x$ MXene-110	1T-MWS/$Ti_3C_2T_x$ MXene-220
1 A g^{-1}	**42**	**163**	**204**	**215**	**284**	**163**
2 A g^{-1}	**37**	**136**	**140**	**154**	**190**	**110**
3 A g^{-1}	**34**	**127**	**124**	**133**	**166**	**95**
5 A g^{-1}	**30**	**116**	**109**	**115**	**145**	**81**
7 A g^{-1}	**27**	**110**	**100**	**102**	**132**	**72**
10 A g^{-1}	**24**	**99**	**90**	**90**	**121**	**63**
15 A g^{-1}	**19**	**89**	**78**	**77**	**107**	**53**
20 A g^{-1}	**15**	**79**	**68**	**66**	**97**	**45**

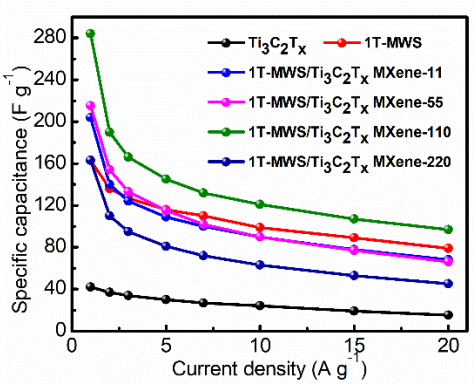

Figure S15. The Specific capacitance of all samples at different current densities of 1, 2, 3, 5, 7, 10, 15 and 20 A g^{-1}.

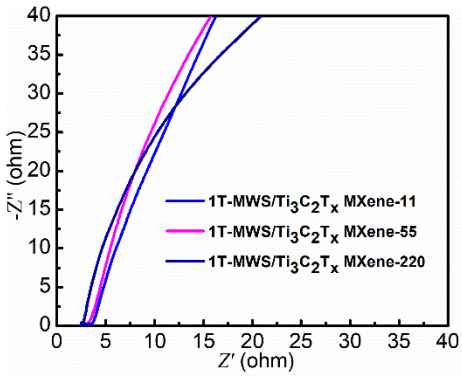

Figure S16. The EIS of 1T-MWS/$Ti_xC_2T_x$ MXene-11, 1T-MWS/$Ti_xC_2T_x$ MXene-55 and 1T-MWS/$Ti_xC_2T_x$ MXene-220.

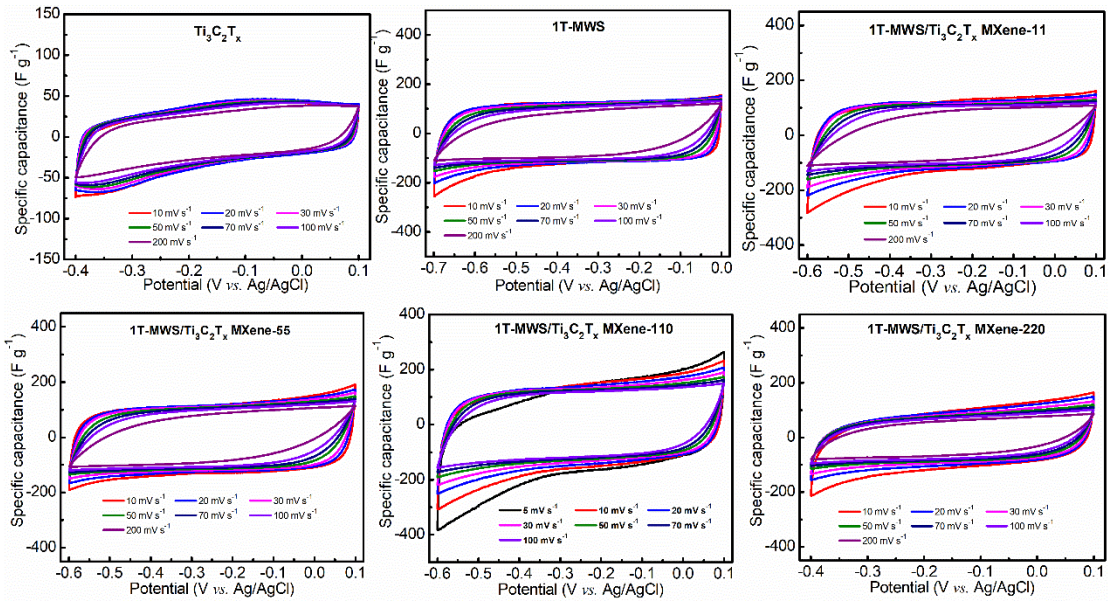

Figure S17. The CV curves of all samples.

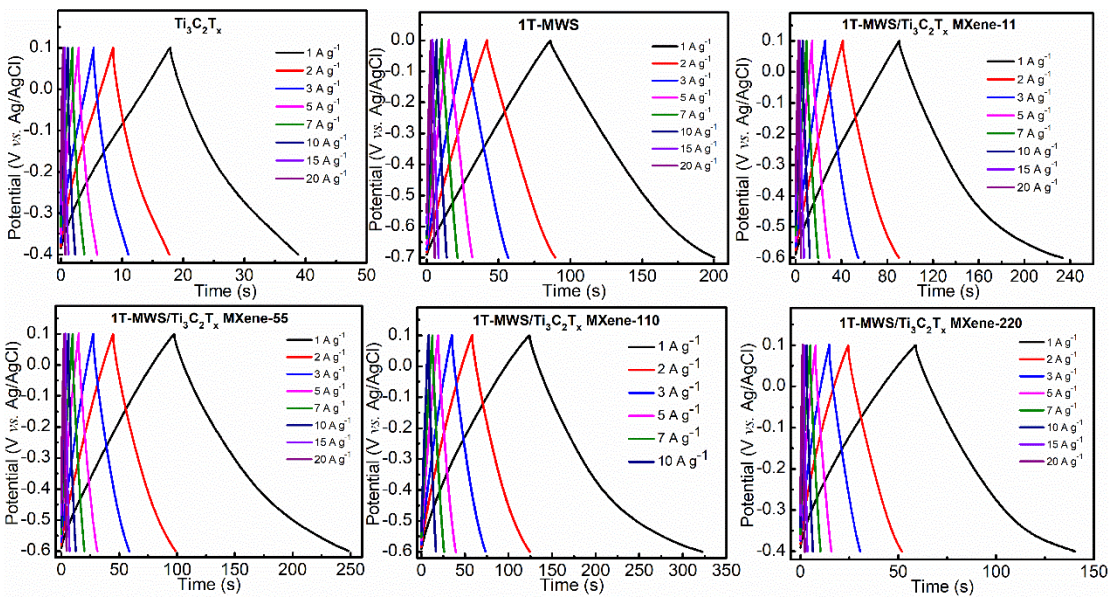

Figure S18. The GCD curves of all samples.

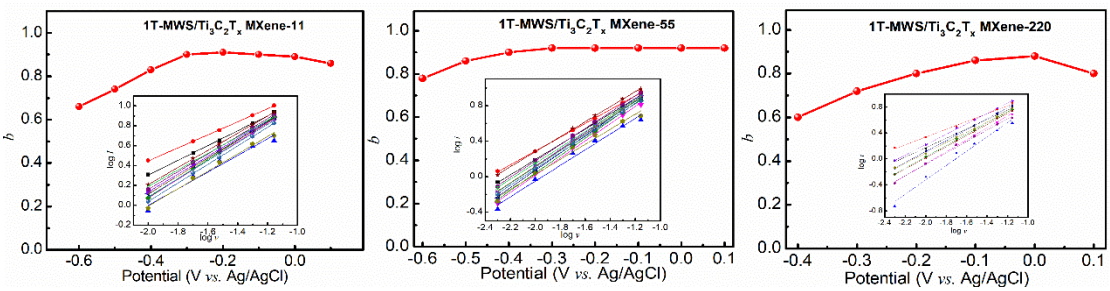

Figure S19. The b values of 1T-MWS/$Ti_3C_2T_x$ MXene-11, 1T-1T-MWS/$Ti_3C_2T_x$ MXene-55 and 1T-MWS/$Ti_3C_2T_x$ MXene-220.

Table S2. The areal capacitance, mass capacitance, energy and power density of the ASSSs devices at different current densities of 1, 2, 3, 5, 7, 10, 15, 20 mA cm^{-2}.

Current density	1 mA cm^{-2}	2 mA cm^{-2}	3 mA cm^{-2}	5 mA cm^{-2}	7 mA cm^{-2}	10 mA cm^{-2}	15 mA cm^{-2}	20 mA cm^{-2}
Areal capacitance	136 mF cm^{-2}	123 mF cm^{-2}	114 mF cm^{-2}	102 mF cm^{-2}	93 mF cm^{-2}	82 mF cm^{-2}	68 mF cm^{-2}	57 mF cm^{-2}
Mass capacitance	64 F g^{-1}	61.6 F g^{-1}	57 F g^{-1}	51 F g^{-1}	46.6 F g^{-1}	41 F g^{-1}	34 F g^{-1}	28.6 F g^{-1}
Energy density	9.3 μWh cm^{-2}	8.4 μWh cm^{-2}	7.8 μWh cm^{-2}	6.9 μWh cm^{-2}	6.3 μWh cm^{-2}	5.6 μWh cm^{-2}	4.6 μWh cm^{-2}	3.9 μWh cm^{-2}
Power density	350 μW cm^{-2}	700 μW cm^{-2}	1050 μW cm^{-2}	1700 μW cm^{-2}	2400 μW cm^{-2}	3500 μW cm^{-2}	5200 μW cm^{-2}	7100 μW cm^{-2}

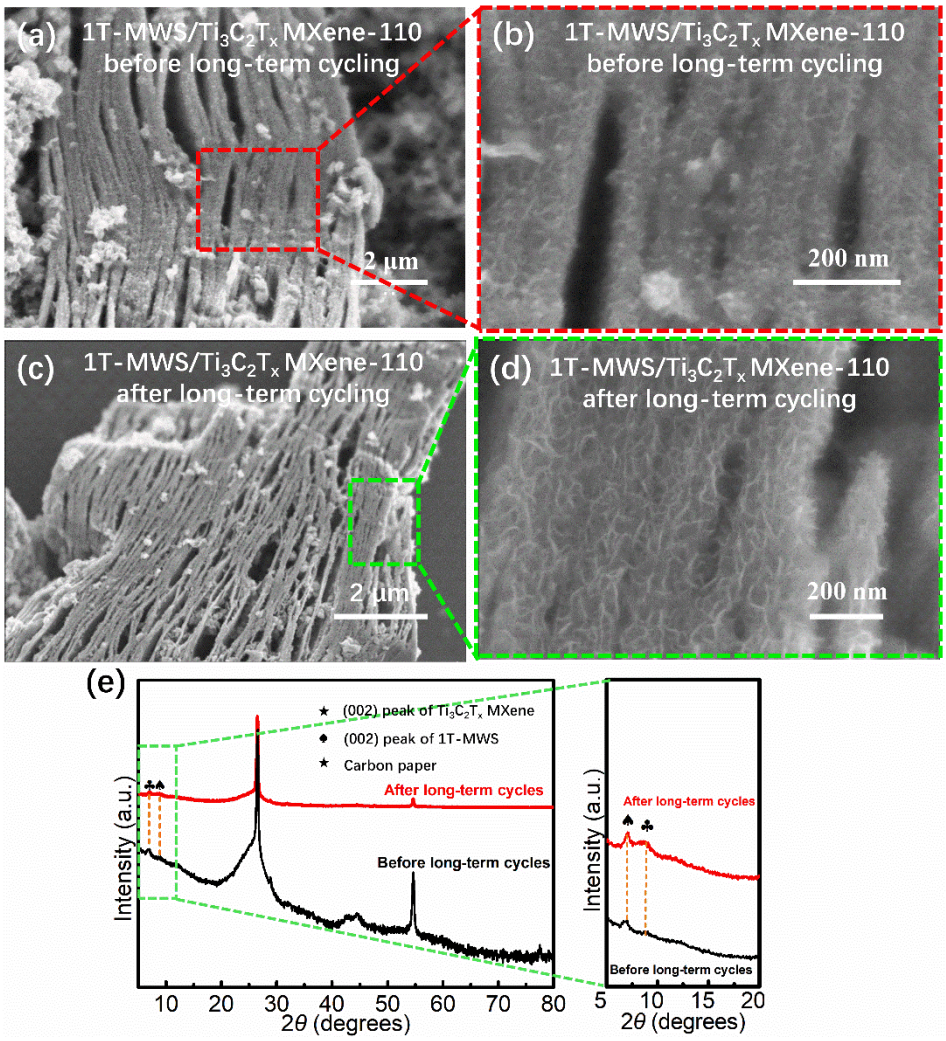

Figure S20. The SEM images and XRD pattern of 1T-MWS/$Ti_3C_2T_x$ MXene-110 electrodes before and after long-term cycling.

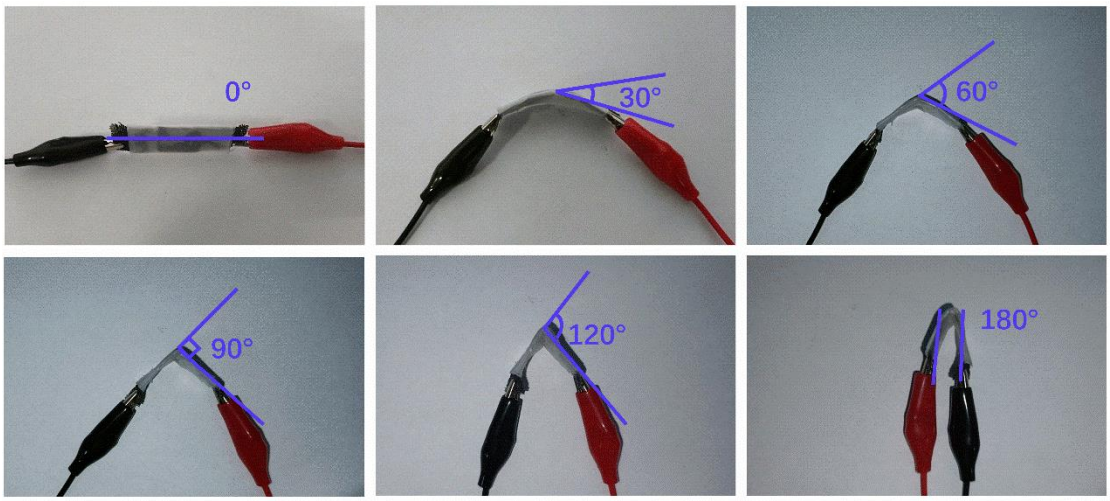

Figure S21. Digital photographs of the symmetric all-solid-state supercapacitors devices bent at different angles of 0°, 30°, 60° and 90° at 20 mV s^{-1}.

Table S3. Comparisons of energy and power density of 1T-MWS/$Ti_3C_2T_x$ MXene-110 based flexible ASSSs with those of advanced flexible devices reported recently.

Flexible device	Energy and power density	Refs.
1T-MWS/$Ti_3C_2T_x$ MXene-110 **1T-MWS/$Ti_3C_2T_x$ MXene-110**	**9.3 μWh cm^{-2} at 350 μW cm^{-2}** **3.9 μWh cm^{-2} at 7100 μW cm^{-2}**	**This work**
RGO/MoS_2/P-10//RGO/MoS_2/P-10	1.44 μWh cm^{-2} at 58 μW cm^{-2}	*Electrochim. Acta* 2020, **330,** 135205.
Laser-induced graphene// laser-induced graphene	4.8 μWh cm^{-2} at 90 μW cm^{-2}	*Electrochim. Acta,* 2020, **357,**136838.
Cu@Ni@NiCoS NFs// Cu@Ni@NiCoS NFs	0.48 μWh cm^{-2} at 11.16 μW cm^{-2}	*Chem. Eng. J.* 2020, **395,**125019.
MnO_2@AuNF//MnO_2@AuNF	0.14 μWh cm^{-2} at 4 μW cm^{-2} 0.05 μWh cm^{-2} at 20 μW cm^{-2}	*J. Mater. Chem. A* 2019, **7,** 10672.
$Co(OH)_2$/AgNWs//$Co(OH)_2$/AgNWs	0.04 μWh cm^{-2} at 2.88 μW cm^{-2}	*ACS Appl. Mater. Interfaces* 2019, **11,** 8992-9001.
$Ti_3C_2T_x$ //carbon nanotube	0.05 μWh cm^{-2} at 2.4 μWh cm^{-2}	*Adv. Mater.* 2017, **29,** 1702678.
RuO_2/PEDOT: PSS//PEDOT: PSS	0.053 μWh cm^{-2} at 147 μWh cm^{-2}	*Nano Energy* 2016, **28,** 495-505.
Ag NW/$Ni(OH)_2$-PEIE// PEDOT: PSS	0.074 μWh cm^{-2} at 3.2 μWh cm^{-2}	*Nano Energy* 2018, **53,** 650-657.
Interdigitated pattern of graphene// Interdigitated pattern of graphene	0.727 μWh cm^{-2} at 83.4 μWh cm^{-2}	*Nano Energy* 2016, **26,** 746-754.
MnHCF-MnOx/ErGO// MnHCF-MnOx/ErGO	2.3 μWh cm^{-2} at 500 μW cm^{-2}	*Adv. Energy Mater.* 2020, **10,** 2000022.
I-$Ti_3C_3T_x$// I-$Ti_3C_3T_x$	0.63 μWh cm^{-2} at 300 μW cm^{-2}	*Adv. Funct. Mater.* 2018, **28,** 1705506.
$Ti_3C_3T_x$// $Ti_3C_3T_x$	1.64 μWh cm^{-2} at 778.3 μW cm^{-2}	*Adv. Mater.* 2020, **32,** 2000716.
N-doped carbon nanotube/Polyurethane// N-doped carbon nanotube/Polyurethane	2.16 μWh cm^{-2} at 50 μW cm^{-2}	*Adv. Energy Mater*. 2017, **7,** 1601814.
Ni−Co DHs/pen ink/nickel/CF// ink-coated nickel/CF	9.75 μWh cm^{-2} at 492.17 μWh cm^{-2} 3.58 μWh cm^{-2} at 1841.1 μWh cm^{-2}	*ACS Appl. Mater. Interfaces* 2017, **9,** 5409-5418.